

Laser-Induced Temperature Jump Electrochemistry on Gold Nanoparticle-Coated Electrodes

Lisa B. Lowe, Scott H. Brewer, Stephan Krämer, Ryan R. Fuieler, Guoguang Qian, Chiamaka O. Agbasi-Porter, Selina Moses, Stefan Franzen, and Daniel L. Feldheim*

Department of Chemistry, North Carolina State University, Raleigh, North Carolina 27695

Received June 13, 2003; E-mail: dan_feldheim@ncsu.edu

We report the effects of laser-induced temperature jumps (LITJs) on the potential of gold nanoparticle-coated indium tin oxide (ITO) electrodes in contact with electrolyte solutions. Lasers have been used previously to effect a temperature change at electrode surfaces. Feldberg and co-workers monitored changes in the open-circuit potential of glass slides coated with a titanium adhesion layer and gold in response to LITJ.¹ Light (1.06 μm) incident on the backside of the electrode (nonsolution side) excited surface plasmons in the titanium. The plasmon excitations relaxed thermally, causing a temperature increase (ca. 3 K in 1 ns) at the gold–solution interface. LITJ has been used to study molecular adsorption on metals,^{1a} heterogeneous electron-transfer kinetics,^{1b,d} and pK_a values of alkanethiol monolayers on gold.^{1c}

Nanometer-sized metal particles such as gold and silver have intense plasmon resonances in the visible region of the electromagnetic spectrum. Excitation of gold nanoparticle plasmons causes rapid local temperature changes which have been used previously to induce polymer gel swelling transitions^{2a,b} and to study the dynamics of melt transitions in nanometer-sized metals.^{2c} Here, we show that plasmon excitations can be employed to change electrode–solution interfacial equilibria. The magnitude of the temperature jump at the gold particle surface was measured with IR thermography and a calibrated redox probe. Biomolecule detection based upon LITJ in metal nanoparticles is also described.

Temperature jumps at an electrode–solution interface alter the open-circuit potential of the electrode versus a reference electrode via primarily four mechanisms:¹ (i) a junction potential induced between the hot electrode and the cold contact, (ii) a junction potential induced between the hot electrical double layer and cold bulk solution (the Soret effect), (iii) a change in the electrical potential (ΔV_{dl}) of the electrode relative to the outer Helmholtz plane due to temperature-induced changes in double-layer capacitance and dipole potentials associated with the double layer, and (iv) a redox potential change (ΔV_{redox}) due to the presence of electron donors and acceptors in solution. The dominant effects are the latter two. As shown below, laser-induced temperature jumps involving gold nanoparticle plasmon excitations are manifested as open-circuit photovoltage changes and photoelectrochemical currents.

LITJ was demonstrated first by attaching 10 nm diameter gold particles to ITO via aminosilane linkers.³ Visible spectroscopy revealed a particle coverage of $2.0 \times 10^{10}/\text{cm}^2$. Current was then monitored during illumination with 532 nm light from a frequency doubled quasi-CW YAG laser (Coherent Antares 76-YAG laser). Figure 1 shows that the largest anodic current was passed when gold nanoparticles were bound to the electrode surface and the electroactive molecule EDTA was present in solution. The photocurrent was observed to vary with applied potential, approaching a maximum value near the oxidation peak potential of EDTA on gold nanoparticle electrodes (0.9 V vs $\text{Ag}_{(s)}/\text{AgCl}$) (Supporting Informa-

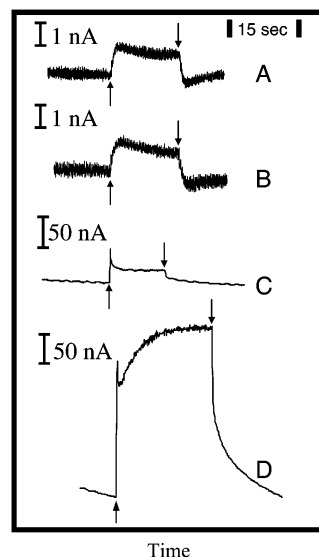


Figure 1. Anodic current versus time for ITO electrodes in (A) 0.1 M phosphate buffer (pH 7.3), (B) 0.1 M phosphate buffer/0.05 M EDTA, and (C) 0.1 M phosphate buffer following adsorption of 10 nm diameter gold particles to the electrode via aminosilane linkers. (D) Electrode from (C) with 0.05 M EDTA added to solution. Up and down arrows denote light on and off, respectively (532 nm light, 0.64 W/cm^2). The potential was held at 0.3 V versus a $\text{Ag}_{(s)}/\text{AgCl}$ reference which was not fixed isothermally.

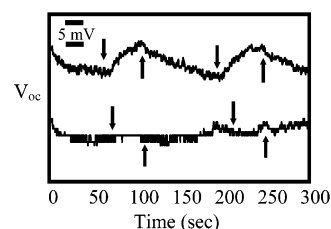


Figure 2. Open-circuit voltage versus time for ITO electrodes in contact with 100 mM ferrocene and 0.1 mM ferrocenium in acetonitrile/0.1 M NaClO_4 . The electrode used to generate the top curve contained 2.0×10^{10} gold nanoparticles cm^{-2} . The bottom curve was ssDNA-coated ITO. Downward and upward arrows indicate light on and off, respectively. (Curves were offset for clarity.)

tion). Close inspection of the data shown in Figure 1D revealed an initial anodic current spike followed by a second rise in anodic current. We ascribe these current changes to the rise in interfacial temperature due to particle plasmon excitation and to the known effects of temperature on ΔV_{redox} , ΔV_{dl} , and heterogeneous electron-transfer rates.¹

The temperature change at the electrode surface was quantified using an internal standard consisting of 100 mM ferrocene and 0.1 mM ferrocenium in acetonitrile (Aldrich). The change in cell potential with temperature for this redox couple was first measured

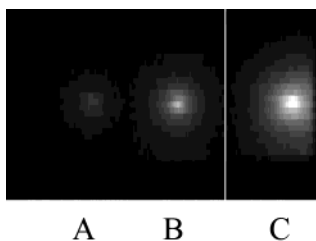


Figure 3. Infrared thermograms (8–12 μm detector) of gold nanoparticle-coated glass slides under irradiation with 532 nm light ($16 \text{ W}/\text{cm}^2$). Particle densities were 1.0×10^{10} , 1.7×10^{10} , and $3.5 \times 10^{10} \text{ cm}^{-2}$ for A, B, and C, with recorded temperatures of 30.5, 35.3, and 42.9 $^{\circ}\text{C}$, respectively. Light-off temperature was 24.6 $^{\circ}\text{C}$. (ΔT for bare glass was $<2 \text{ }^{\circ}\text{C}$.)

using a two-compartment electrochemical cell and hot plate and was determined to be $0.35 \text{ mV } ^{\circ}\text{C}^{-1}$. When the solution was placed in contact with a nanoparticle-coated ITO electrode and irradiated at 532 nm, a 9 mV change was recorded (Figure 2). This value corresponds to an interfacial ΔT of 25 $^{\circ}\text{C}$ induced by the LITJ effect.

The interfacial temperature change at nanoparticle-coated ITO electrodes was confirmed using infrared (IR) thermography (Inframetrics 740). The interfacial temperature depended upon irradiation time (not shown) and nanoparticle surface coverage (Figure 3). Following 30 s of irradiation, a surface temperature of 42.9 $^{\circ}\text{C}$ was measured for a coverage of 3.5×10^{10} particles cm^{-2} . Using IR thermography, we have recorded temperature changes of 2.5 $^{\circ}\text{C}$ for as few as ca. 10^5 nanoparticles (10^6 cm^{-2}).

Finally, the LITJ effect can be exploited in the form of a new type of chemical sensor in which a binding event between an ITO-bound analyte probe molecule and a gold-labeled target molecule is transduced photoelectrochemically. As proof-of-principle, complementary 20 bp ssDNA sequences were attached to ITO and 10 nm diameter gold nanoparticles (Supporting Information). Figure 4 shows that hybridization events between nanoparticles and the surface can be detected with the LITJ photoelectrochemical response. Surface hybridization has been detected with signals at least twice the background for ssDNA-modified gold nanoparticle solution concentrations ranging from 100 fM to 1.0 nM.

In conclusion, LITJ involving gold nanoparticles is important because it may increase background signals in applications involving solar energy conversion.⁴ Alternatively, the LITJ effect could be a useful new electrochemical tool for applications in bioanalytical chemistry. In contrast to direct electroanalysis techniques, LITJ electrochemistry does not depend on intimate contact between a redox label and the electrode surface. Thus, large DNA strands or proteins that place a nanoparticle label tens to hundreds of nanometers from the surface will still produce a LITJ response at the electrode–solution interface.

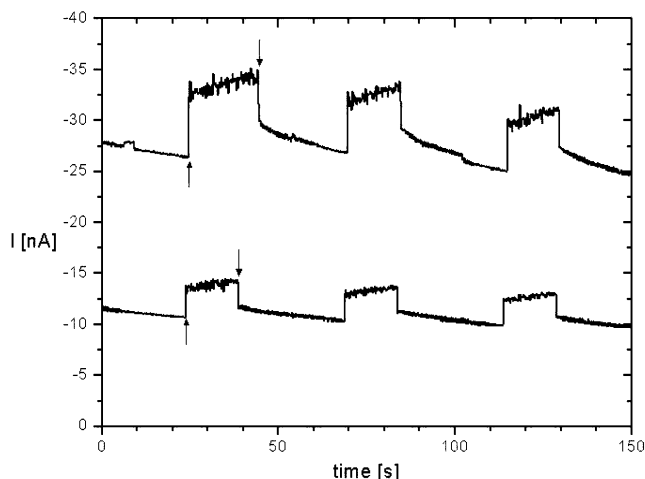


Figure 4. Anodic current versus time for an ITO electrode in 0.1 M phosphate buffer/0.05 M EDTA following adsorption of 10 nm diameter gold particles to the electrode via DNA hybridization. The potential was held at 0.5 V versus Ag/AgCl. Top trace: ssDNA/gold nanoparticle conjugates hybridized from a 100 fM solution as described in ref 5. Bottom trace: ssDNA probe strands on ITO. Up and down arrows denote light on and off, respectively. Note $I(\text{light on}) - I(\text{light off})$ in the top trace is $\sim 2\times$ that in the bottom trace.

Acknowledgment. The authors thank Drs. Tim Woudenberg and Tim Liu at Applied Biosystems, Inc., for supplying the infrared camera and financial support. The authors also thank Dr. Stephen Feldberg for helpful discussions.

Supporting Information Available: Procedures for modifying ITO with ssDNA and characterization by X-ray photoelectron spectroscopy (PDF). This material is available free of charge via the Internet at <http://pubs.acs.org>.

References

- (1) (a) Smalley, J. F.; Geng, L.; Feldberg, S. W. *J. Electroanal. Chem.* **1993**, 356, 181. (b) Smalley, J. F.; Krishnan, C. V.; Goldman, M.; Feldberg, S. W. *J. Electroanal. Chem.* **1988**, 248, 255. (c) Smalley, J. F.; Chalfant, K.; Feldberg, S. W.; Nahir, T. M.; Bowden, E. F. *J. Phys. Chem. B* **1999**, 103, 1676. (d) Smalley, J. F.; Geng, L.; Chen, A.; Feldberg, S. W.; Lewis, N. S.; Cali, G. *J. Electroanal. Chem.* **2003**, 549, 13.
- (2) (a) Jones, C. D.; Lyon, L. A. *J. Am. Chem. Soc.* **2003**, 125, 460. (b) Sershen, S. R.; Westcott, S. L.; Halas, N. J.; West, J. L. *J. Biomed. Mater. Res.* **2000**, 51, 293. (c) Link, S.; Burda, C.; Nikoobakat, B.; El-Sayed, M. A. *J. Phys. Chem. B* **2000**, 104, 6152.
- (3) Grabar, K. C.; Smith, P. C.; Musick, M. D.; Davis, J. A.; Walter, D. G.; Jackson, M. A.; Guthrie, A. P.; Natan, M. J. *J. Am. Chem. Soc.* **1996**, 118, 1148.
- (4) (a) Yamada, S.; Koide, U.; Matsuo, Y. *J. Electroanal. Chem.* **1997**, 426, 23. (b) Lahav, L.; Geleg-Shabtai, V.; Wasserman, J.; Katz, E.; Willner, I.; Durr, H. Hu, Y.-Z.; Bossmann, S. H. *J. Am. Chem. Soc.* **2000**, 122, 11480.
- (5) (a) Sauthier, M. L.; Carroll, R. L.; Gorman, C. B.; Franzen, S. *Langmuir* **2002**, 18, 1825. (b) Brewer, S. H.; Brown, D. A.; Franzen, S. *Langmuir* **2002**, 18, 6857–6865.

JA036672H